Full Paper

New Phytologist

DLK2 regulates arbuscule hyphal branching during arbuscular mycorrhizal symbiosis

Tania Ho-Plágaro[1], Rafael J. L. Morcillo[2], María Isabel Tamayo-Navarrete[1], Raúl Huertas[3], Nuria Molinero-Rosales[1], Juan Antonio López-Ráez[1], Alberto P. Macho[2] and José Manuel García-Garrido[1]

[1]Department of Soil Microbiology and Symbiotic Systems, Estación Experimental del Zaidín (EEZ), CSIC, Calle Profesor Albareda n°1, Granada 18008, Spain; [2]Shanghai Center for Plant Stress Biology, CAS Center for Excellence in Molecular Plant Sciences, Shanghai Institutes of Biological Sciences, Chinese Academy of Sciences, Shanghai 201602, China; [3]Noble Research Institute LLC, 2510 Sam Noble Parkway, Ardmore, OK 73401, USA

Author for correspondence:
José Manuel García Garrido
Email: josemanuel.garcia@eez.csic.es

Received: *24 July 2020*
Accepted: *2 September 2020*

New Phytologist (2021) **229:** 548–562
doi: 10.1111/nph.16938

Key words: arbuscular mycorrhiza, arbuscule formation, butenolide signaling, DLK2 protein, tomato.

Summary

- D14 and KAI2 receptors enable plants to distinguish between strigolactones (SLs) and karrikins (KARs), respectively, in order to trigger appropriate environmental and developmental responses. Both receptors are related to the regulation of arbuscular mycorrhiza (AM) formation and are members of the RsbQ-like family of α,β-hydrolases. DLK2 proteins, whose function remains unknown, constitute a third clade from the RsbQ-like protein family. We investigated whether the tomato *SlDLK2* is a new regulatory component in the AM symbiosis.
- Genetic approaches were conducted to analyze *SlDLK2* expression and to understand SlDLK2 function in AM symbiosis.
- We show that *SlDLK2* expression in roots is AM-dependent and is associated with cells containing arbuscules. *SlDLK2* ectopic expression arrests arbuscule branching and downregulates AM-responsive genes, even in the absence of symbiosis; while the opposite effect was observed upon *SlDLK2* silencing. Moreover, *SlDLK2* overexpression in *Medicago truncatula* roots showed the same altered phenotype observed in tomato roots. Interestingly, SlDLK2 interacts with DELLA, a protein that regulates arbuscule formation/degradation in AM roots.
- We propose that SlDLK2 is a new component of the complex plant-mediated mechanism regulating the life cycle of arbuscules in AM symbiosis.

Introduction

Strigolactones (SLs) and karrikins (KARs), two molecules bearing essential butenolide moieties, play important biochemical and physiological roles in plants. Since SLs are identified as both rhizospheric signals to mycorrhizal fungi (Akiyama *et al.*, 2005; Akiyama *et al.*, 2010) and hormonal signals within the plant body (Gomez-Roldan *et al.*, 2008; Umehara *et al.*, 2010), a large number of publications have shown novel and diverse functions for SLs in plants, many of which come from the interpretation of mutant phenotypes. By contrast, KARs are abiotic and exogenous molecules of more limited occurrence derived from partial plant combustion. KARs are reported to promote seed germination and seedling establishment, and then are considered as adaptive chemical signals that improve seedling recruitment and establishment after fire events (Flematti *et al.*, 2004; Nelson *et al.*, 2010).

KARRIKIN INSENSITIVE2 (KAI2) – also known as HTL or D14-LIKE (D14L) – and DWARF14 (D14) proteins enable plants to distinguish between KARs and SLs, respectively, in order to trigger appropriate environmental and developmental responses (Mindrebo *et al.*, 2016). KAI2 and D14 are α,β-hydrolase fold proteins closely related, and are members of the RsbQ-like family (Mindrebo *et al.*, 2016), also named as DWARF14 family (Waters *et al.*, 2012) or the KAI2/D14 family (Bennett *et al.*, 2016). Based on current data, D14 and KAI2 proteins themselves have a very similar overall structure (a compact α/β-fold hydrolase structure of a β-sheet core flanked by α-helices). These proteins contain a deep binding pocket, containing a conserved catalytic triad of serine/histidine/aspartate, with a V shaped cap covering the pocket. The differences in pocket shape and size between D14 and KAI2 proteins are features that influence ligand specificity (Machin *et al.*, 2020).

The DWARF14-LIKE2 (DLK2) proteins constitute a third divergent clade of the RsbQ-like family, and *DLK2* gene expression is conventionally used as a marker for SL and KAR activity (Waters *et al.*, 2012; Sun *et al.*, 2016). Although the DLK2 proteins are structurally very similar to D14 and KAI2, its function is mostly unknown. Apart from regulating *Arabidopsis* seedling photomorphogenesis, no other physiological role has been assigned to DLK2 to date (Végh *et al.*, 2017). Since *dlk2* mutants are essentially aphenotypic, their role could be associated with physiological processes that are not easily identifiable during plant development (Waters *et al.*, 2012; Bennett *et al.*, 2016; Végh *et al.*, 2017).

Today, it is established that the catalytic activities of SL/KAR α,β-hydrolase receptors are important but that hydrolysis is not

required to produce a bioactive molecule. In some cases, this cleavage induces the interaction with the DELLA transcription factor, as it has been shown for the SL receptor D14 of rice (Nakamura *et al.*, 2013). Moreover, SL and KAR signaling involve subsequent regulated proteolytic degradation (like in the auxin, gibberellin and jasmonate signaling pathways) (Wang *et al.*, 2020) mediated by MAX2, an F-box protein belonging to an SCF-type E3 ubiquitin ligase complex (Stirnberg *et al.*, 2002, 2007; Wang *et al.*, 2020).

Arbuscular mycorrhiza (AM), established between the endosymbiotic AM fungi and higher plants, is the most widespread symbiosis in the plant kingdom. In the cortical cells of the roots, the AM fungi develops specialized intraradical and highly branched structures, called arbuscules, where bidirectional exchange of nutrients between plant and fungi partners occurs (Smith & Read, 2008; Luginbuehl & Oldroyd, 2017). During the establishment of the symbiosis, the interaction is highly regulated by both partners at the cellular, molecular and genetic levels. Host plant cells regulate the development and functioning of arbuscules by a complex transcriptional reprogramming and hormone signaling, such as the upregulation of genes encoding GRAS transcription factors and the participation of DELLA-mediated gibberellins (MacLean *et al.*, 2017; Pimprikar & Gutjahr, 2018).

Recent discoveries have begun to elucidate distinct roles for SL-related components in AM symbiosis. It has become evident that SLs are involved in controlling pre-symbiotic events in AM formation (Akiyama *et al.*, 2005), and that rice KAI2 (KAR receptor) is essential for the perception of symbiotic signaling required for mycorrhizal association (Gutjahr *et al.*, 2015a). Moreover, the expression of SL biosynthesis genes is partly upregulated in AM colonized roots (Kobae *et al.*, 2018), and several studies have shown that mutants or antisense lines impaired in SL biosynthesis or transport exhibit reduced mycorrhization, although morphology of intercellular hyphae and arbuscules was not affected (Gomez-Roldan *et al.*, 2008; Koltai *et al.*, 2010; Vogel *et al.*, 2010; Kretzschmar *et al.*, 2012; Yoshida *et al.*, 2012). Recent observations from Kobae *et al.* (2018) established that SL biosynthetic genes are also required for efficient hypopodium formation, suggesting a role of SLs in both the pre-symbiotic chemical dialog and the subsequent hyphal entry into the roots.

Then, it is clear that the SL and KAR receptors, D14 and KAI2, respectively, are in a certain way related to the regulation of AM symbiosis. As before mentioned, these two proteins belong to the RsbQ-like α,β-hydrolases family that is divided in three protein clades: D14, KA2 and DLK2 (Delaux *et al.*, 2012; Hamiaux *et al.*, 2012; Waters *et al.*, 2012). Here, we have identified a tomato gene encoding a DWARF14-LIKE2 (SlDLK2) protein as a member of the third clade of the family. This gene was found to be highly upregulated in arbuscular mycorrhizal tomato roots in the microarray hybridizations and data analysis carried out previously by García Garrido *et al.* (2010) and López-Ráez *et al.* (2010). In addition, García Garrido *et al.* (2010) also observed that the *SlDLK2* induction was highly reduced in mycorrhizal roots of *sitiens*, an ABA-deficient tomato mutant with an impaired AM formation (Herrera-Medina *et al.*, 2007), which suggests that *SlDLK2* hydrolase gene could play an essential role in the AM symbiosis formation. Here we have shown that *SlDLK2* expression in roots is AM-dependent and is associated with cells containing arbuscules. We have demonstrated that SlDLK2 interacts with DELLA protein and *SlDLK2* overexpression (OE) arrests arbuscule branching and downregulates AM-related genes. Our results as a whole suggest that this new regulatory component acts as a negative signaling regulator of arbuscule branching.

Materials and Methods

Plant growth and AM inoculation

Solanum lycopersicum seeds were surface sterilized with a 5 min soaking using 2.35% w/v sodium hypochlorite, subjected to shaking at room temperature for 1 d in the dark, and germinated on a sterilized moistened filter paper for 4 d at 25°C in the dark. Germinated seeds were placed on vermiculite for hypocotyl elongation for 1 wk. Each seedling was transferred to a 500-ml pot containing an autoclave-sterilized (20 min at 120°C) mixture of expanded clay, washed vermiculite and coconut fiber (2 : 2 : 1, v/v). In the AM inoculated treatments, the plants were inoculated with a piece of monoxenic culture in Gel-Gro medium produced according to Chabot *et al.* (1992), containing *c.* 50 spores of *Rhizophagus irregularis* (DAOM 197198) and infected carrot roots. For the noninoculated treatment a piece of Gel-Gro medium containing only uninfected carrot roots was used. Plant growth took place in a growth chamber (day : night cycle, 16 h : 8 h, 24°C : 20°C; relative humidity 50%).

One week after planting and weekly thereafter, the pots were given 20 ml of a modified Long Ashton nutrient solution (Hewitt, 1966) containing 25% (325 μM) of the standard phosphorous concentration (1.3 mM) to prevent mycorrhizal inhibition as a result of excess of phosphorous. In the case of nonmycorrhizal plants, the same modified Long Ashton solution was used. Plants were harvested at different times after inoculation. The root system was washed and rinsed several times with tap water, and used for the different measurements according to the nature of the experiments. In each experiment, at least five independent biological replicates were analyzed per treatment.

Estimation of root colonization by AM fungus

The nonvital trypan blue histochemical staining procedure was used according to the Phillips & Hayman (1970) method. Stained roots were observed with a light microscope, and the intensity of root cortex colonization by AM fungus was determined as described by Trouvelot (1986) using the MYCOCALC software (http://www.dijon.inra.fr/mychintec/Mycocalc-prg/download.html). The parameters measured were frequency of colonization (%F), intensity of colonization (%M) and arbuscular abundance (%A) along the whole root length. At least five microscope slides were analyzed per biological replicate, and each slide contained 30 root pieces of 1 cm. Alternatively, 120 root

intersects from each of these slides were analyzed to sort the prevalence of arbuscules from three morphologically different developmental stages, as well as the presence or absence of vesicles.

Expression analysis of RsbQ α,β-hydrolase genes in tomato organs

Gene expression from all the six RsbQ α,β-hydrolase tomato genes was analyzed by quantitative reverse transcription polymerase chain reaction (RT-qPCR) in various organs of *S. lycopersicum* cv Moneymaker plants. Tomato plants of 100 d old were used to analyze the corresponding gene expression in roots, leaves, young flower buds, mature flower buds, open flowers, green fruits and young stems. The 125 d old plants were used to measure gene expression in developing fruits turning red, mature fruits in red and seeds.

Promoter sequence identification

Since, at the time of this analysis, *SlDLK2* promoter sequences had not yet been assembled in the tomato genome version SL4.0 (Hosmani *et al.*, 2019), promoter sequences were obtained using the Universal Genome Walker 2.0 Kit (Clontech, Mountain View, CA, USA), following the manufacturer instructions. Genomic DNA from *S. lycopersicum* cv Moneymaker was extracted using the DNAeasy Plant Mini Kit (Qiagen, Hilden, Germany), digested with four restriction enzymes (DraI, EcoRV, PvuII and StuI), purified, and ligated to the Genome Walker adapters provided with the Universal Genome Walker kit. A primary PCR with GSP1 and Ap1 primers, and a secondary (or 'nested') PCR with GSP2 and Ap2 primers, were performed. Primers used were two designed reverse Gene Specific Primers (GSP1 5′CATCAGCAAAAGGCTCATAGGAGGAGTA3′ and GSP2 5′CCCAAACTGATTGATCTCCTCCATATCC3′), and two Adaptator Specific Primers (Ap1 and Ap2) provided in the kit. PCR products were purified and sequenced, and the fragment corresponding to the *SlDLK2* promoter (a 1560-bp fragment immediately upstream of the start codon of *SlDLK2*) was selected for cloning. Lately, the *SlDLK2* promoter sequence has been verified against the latest available tomato Genome Version, SL4.0.

Plasmid construction and hairy root transformation

Full-length cDNA gene sequence of *SlDLK2* (Solyc05g018413.1.1, according to the updated ITAG 4.0 annotation), and a 235 bp-*SlDLK2* RNAi fragment were amplified from *S. lycopersicum* cDNA of roots infected by the AM fungus *R. irregularis*. The putative promoter of *SlDLK2* was obtained from genomic DNA of *S. lycopersicum* cv Moneymaker. Amplifications were carried out by PCR using the iProof High Fidelity DNA-polymerase (BioRad, Hercules, CA, USA) and specific primers (Supporting Information Table S1). PCR fragments were introduced in pENTR/D-TOPO (Invitrogen, Carlsbad, CA, USA) vector and sequenced. pENTR/D-TOPO containing the *SlDLK2* gene, an RNAi *SlDLK2* fragment and the *SlDLK2* promoter, were subsequently recombined into pUBIcGFP-DR (Kryvoruchko *et al.*, 2016), pK7GWIWG2_II-RedRoot (http://gateway.psb.ugent.be) and pBGWFS7:: pAtUbq10:: DsRed (modified from Karimi *et al.* (2002)) vectors, respectively, using the GATEWAY technology (Invitrogen).

For hairy root transformation, *Agrobacterium rhizogenes* MSU440 cultures harboring the corresponding overexpression, RNA interference (RNAi), and promoter-GUS constructs, were used to transform *S. lycopersicum* cv Moneymaker plantlets according to Ho-Plágaro *et al.* (2018). Composite plants were transferred to pots and followed the same plant growth conditions as explained earlier. Screening and selection of DsRed (transformed) roots was done by observation under a fluorescent stereomicroscope Leica M165F.

For protein–protein interaction assays, the *SlDLK2* and *SlGAI1* gene fragments from *S. lycopersicum* were amplified and cloned into the pENTR-D-TOPO vector (Thermo Scientific, Waltham, MA, USA). For the co-immunoprecipitation assay, these *SlDLK2* and *SlGAI1* gene fragments were subcloned into the pK7FWG2.0 (Karimi *et al.*, 2002) and pTA7001 (Anders & Huber, 2010) gateway binary vectors in order to generate a C-terminal fusion of *SlDLK2* to green fluorescent protein (GFP), and a dexamethasone inducible C-terminal fusion of *SlGAI1* to a 3xFlag tag, respectively. For split luciferase assays, *SlDLK2* and *SlGAI1* genes fragments were subcloned into pGWB-NLuc to generate a C-terminal fusion of partial (N-terminal) luciferase protein (SlDLK2-NLuc), and into pGWB-CLuc to generate a N-terminal fusion of partial (C-terminal) luciferase protein (CLuc-SlGAI1), respectively. *SlWRKY75* gene from *S. lycopersicum* was sublconed into pGWB-NLuc to generate a C-terminal fusion of partial (N-terminal) luciferase protein (SlWRKY75-NLuc) (Wang *et al.*, 2018). All constructs were transformed into *A. tumefaciens GV3101*.

Spatial analysis of *SlDLK2* promoter activity

In order to localize the expression of *SlDLK2* gene, AM inoculated and noninoculated transgenic roots carrying the *SlDLK2* promoter-GUS fusion were used, based on a technique originally developed by Jefferson (1989). Roots transformed with the empty vector were used as a negative control. Roots transformed by a *PT4* promoter-GUS fusion were used as a positive control in the same manner as Ho-Plágaro *et al.* (2018). Hairy roots carrying the promoter-GUS fusions were vacuum-infiltrated with a GUS staining solution composed of 0.05 M sodium phosphate buffer, 1 mM potassium ferrocyanide, 1 mM potassium ferricyanide, 0.05% Triton X-100, 10.6 mM ethylene diamine tetraacetic acid (EDTA)-sodium salt and 5μg ml^{-1} X-gluc cyclohexylammonium salt (previously dissolved in *N,N*-dimethylformamide) for 30 min to improve the penetration of the substrate. Then, the tissues were incubated in the dark at 37°C from 1 h to overnight or until the staining was satisfactory in the same staining solution.

In order to stain the AM fungal structures, the inoculated roots were embedded in 4% agarose blocks and 60 μm transverse sections were cut on a vibratome (Leica VT1200S). Root sections

were vacuum-infiltrated with 10 μg ml^{-1} WGA-Alexa Fluor 488 conjugate (Molecular Probes, Eugene, OR, USA) in PBS 1X for 60 min in the dark and analyzed under an inverted transmission microscope (Leica DMI600B).

RNA extractions and gene expression quantification

For the RT-qPCR experiments, representative root samples from each root system were collected, immediately frozen in liquid nitrogen, and stored at −80°C until RNA extraction. Total RNA was isolated from about 0.2 g – samples using the RNeasy Plant Mini Kit (Qiagen) following the manufacturer's instructions, and treated with RNase-Free DNase. 1 μg of DNAse-treated RNA was reverse-transcribed into cDNA using the iScriptTM cDNA synthesis kit (BioRad) following the supplier's protocol. For the qPCR, it was prepared a 20 μl PCR reaction containing 1 μl of diluted cDNA (1 : 10), 10 μl 2× SYBR Green Supermix (BioRad) and 200 nM of each primer using a 96-well plate. A negative control with the RNA sample before reverse-transcription was used in order to confirm that the samples were free from DNA contaminations. PCR program consisted of a 3 min incubation at 95°C, followed by 35 cycles of 30 s at 95°C, 30 s at 58–63°C, and 30 s at 72°C. The specificity of the PCR amplification procedure was checked using a melting curve after the final PCR cycle (70 steps of 30 s, from 60 to 95°C, at a heating rate of 0.5°C). Experiments were carried out on three biological replicates, and the threshold cycle (Ct) value for each biological replicate was determined from three technical replicates. The relative transcription levels were calculated by using the $2^{-\Delta\Delta Ct}$ method (Livak & Schmittgen, 2001). The Ct values of all genes were normalized to the geometric mean of Ct values from the *LeEF-1α* (accession no. X14449) and actin (NM_001321306.1) housekeeping genes.

The RT-qPCR data for each gene were shown as relative expression with respect to the control treatment ('reference treatment') to which it was assigned an expression value of 1. The reference treatment generally corresponded to the non-AM inoculated treatment. All genes whose transcript abundance was measured by RT-qPCR and the corresponding primers used are listed in Table S2.

Phylogenetic analysis

Using the on-line BLASTP server at the National Center for Biotechnology Information (NCBI) (www.ncbi.nlm.nih.gov) with all default settings, amino acid sequence of SlDLK2 was subjected to a homology search against a series of selected dicot and monocot species. Blast output sequences with an alignment score ≥ 200 were considered as putative homologs. These proteins, together with other putative homologs that have been previously characterized in the literature were selected for further alignment using CLUSTAL OMEGA (Sievers *et al.*, 2011). Phylogenetic relationships were determined with MEGA7 software (Kumar *et al.*, 2016) to create a maximum-likelihood (ML) tree using Jones–Taylor–Thornton (JTT) as the amino acid substitution model and the nearest-neighbor-interchange (NNI) heuristic method to improve the likelihood of the tree. The partial deletion (95%) mode was used for the treatment of gaps and missing data. 100 bootstrap replications were performed. The tree was rooted on the RsbQ from *Bacillus subtilis*.

RNA preparation and Illumina sequencing

Root pools from two independent experiments were collected for the RNA-seq analysis. For the first experiment, related to transcriptional changes undergoing arbuscular mycorrhization, three pools from noninoculated plants and three pools from AM-inoculated plants (35.88 ± 4.93% mycorrhizal colonization) were used. For the second experiment, concerning transcriptomic alterations upon *SlDLK2* OE in noninoculated roots, three root pools from control plants transformed with the empty vector and three pools of *SlDLK2* OE composite plants were used. Each pool was composed of a representative mixture of two root systems from two composite plants. Total RNA was extracted using the Rneasy Plant Mini Kit (Qiagen). The quality and quantity of total RNA samples were assessed using a NanoDrop 1000 spectrophotometer (Thermo Scientific) and samples were normalized at the same concentration (6 μg, 300 ng μl^{-1}). Later, samples were sent to Sistemas Genómicos SL (Paterna, Valencia, Spain) for cDNA library preparation and sequencing using an Illumina HiSeq1000 machine.

RNA-seq sequence processing

The TOPHAT v.2.1.0 algorithm (Trapnell *et al.*, 2009) was used to align reads from the RNA-Seq experiment to the Tomato Genome Reference Sequence SL3.0 provided by the Sol Genomics consortium at (https://solgenomics.net/organism/Solanum_lycopersicum/genome), using the last ITAG 3.10 annotation. Then, low quality reads were removed from the map through Picard Tools (http://picard.sourceforge.net), and high quality reads were selected for assembly and identification through Bayesian inference using the CUFFLINKS v.2.2.1 algorithm proposed by Trapnell *et al.* (2010). Gene quantification process was performed by the HTSEQ-COUNT 0.6.1p1 tool (Anders *et al.*, 2015). Isoform quantification and differential expression was carried out through the DESEQ2 method (Anders *et al.*, 2015).

The RNA-seq data have been deposited in the NCBI Short Read Archive (SRA) with accession nos. PRJNA509606; PRJNA523214.

Co-immunoprecipitation assay

Agrobacterium-mediated transient expression in *Nicotiana benthamiana* was performed as described previously (Li, 2011). Before infiltration, the bacterial suspension was adjusted to a final optical density at 600 nm (OD_{600}) of 0.5. *Nicotiana benthamiana* leaves were co-infiltrated with *A. tumefaciens* GV3101 carrying plasmids to induce the expression of *SlDLK2* (pK7FWG2.0) and *SlGAI1* (pTA7001). Leaves co-infiltrated with GV3101 carrying *GFP* (pGW505) and *SlGAI1* (pTA7001) were used as negative controls. *SlGAI1*-3xFlag expression was induced by dexamethasone for

24 h. Furthermore, 3–5 g of *N. benthamiana* leaf materials at 48 h after co-infiltration were frozen and ground in liquid nitrogen for protein extraction, and immunoprecipitation was performed with GFP-trap beads according to Sang *et al.* (2018). Total proteins were extracted using protein extraction buffer (100 mM Tris-HCl, pH 7.5, 150 mM NaCl, 10% glycerol, 5 mM EDTA, 10 mm dithiothreitol (DTT), 2 mM phenylmethylsulfonyl fluoride (PMSF), 0.5% (v/v) IGEPAL (IGEPAL CA-630), 1% (v/v) Plant Protease Inhibitor cocktail (Sigma, St Louis, MO, USA)). Extracts were mixed for 15 min at 4°C and centrifuged at 15 000 ***g*** for 15 min at 4°C to completely remove debris. GFP-trap beads (ChromoTek, Martinsried, Germany) were added to the supernatant and incubated for 1 h at 4 °C with slow but constant rotation. Conjugated beads were washed three times with 1 ml cold wash buffer (100 mM Tris-HCl, pH 7.5, 150 mM sodium chloride (NaCl), 10% glycerol, 2 mM DTT, 1% (v/v) IGEPAL, 1% (v/v) Plant Protease Inhibitor cocktail (Sigma)) and once with wash buffer 0.5% IGEPAL before stripping interacting proteins from the beads by boiling in 50 µl Laemmli sample buffer (BioRad) for 5 min. Immunoprecipitated proteins were separated on precast sodium dodecyl sulfate-polyacrylamide gel electrophoresis (SDS-PAGE) gels (BioRad) and Western blot was performed using the anti-FLAG (Abmart, Berkeley Heights, NJ, USA) and anti-GFP (Abiocode, Agoura Hills, CA, USA) primary antibodies.

Split-luciferase assay

Nicotiana benthamiana leaves were co-infiltrated with *A. tumefaciens* GV3101 carrying plasmids to induce the expression of SlDLK2-NLuc and CLuc-SlGAI1. Leaves infiltrated with GV3101 carrying SlWRKY75-NLuc and CLuc-SlGAI1 were used as negative controls. Briefly, 50 mM luciferin was infiltrated and the materials were kept in the dark for 3 to 5 min to quench the fluorescence. Total protein was extracted from equal amounts of *N. benthamiana* leaves and separated on precast sodium SDS-PAGE gels, similarly as described earlier (co-immunoprecipitation assay). Protein blot was hybridized with the rabbit anti-full-length firefly LUC antibodies (Sigma), which react with both the N-terminal and C-terminal firefly LUC fragments. LB 985 *in vivo* Plant Imaging System (Berthold Technologies, Bad Wildbad, Germany) was used to capture the LUC image, using 1 min as exposure time for all images taken. Quantification of LUC signal (Average [ph/s], photons emitted/area) was calculated with INDIGO™ software (Berthold Technologies). The protein blot was stained with Coomassie brilliant blue to verify equal loading.

Statistical analysis

When two means were compared, the data was analyzed using a two tailed Student's *t*-test. For comparisons among all means, a one-way or two-way analysis of variance (ANOVA) was performed followed by the least significant difference (LSD) multiple comparison test. The Graphpad PRISM v.6.01 (Graphpad Software, San Diego, CA, USA) was used to determine statistical significance. Differences at $P < 0.05$ were considered significant. Data represent the mean ± SE.

Results

Phylogenetic and expression analysis of the Rsb-Q-like α,β-hydrolase family in tomato

Phylogenetic analysis showed that the SlDLK2 protein belongs to a third clade of RsbQ-like α,β-hydrolases (Fig. S1) of unknown function, and appears as a divergent clade from the D14/KAI2 groups, similarly to Hamiaux *et al.* (2012). This analysis revealed the presence of five other tomato α,β-hydrolases belonging to the RsbQ-like group, in addition to SlDLK2 (Fig. S1). Only one tomato α,β-hydrolase, the putative SlD14 protein, belongs to the D14 clade, while two pairs of α,β-hydrolases were found in the KAI2 clade. One pair is constituted by two proteins named here as 'SlKAI2**c**A' and 'SlKAI2**c**B' (KAI2 **c**onserved), because they are the closest tomato homologs to the previously characterized KAR1 receptors AtD14L and OsD14L (Kagiyama *et al.*, 2013; Gutjahr *et al.*, 2015a). The other pair (KAI2 **i**ntermediate pair), is composed by the 'SlKAI2**i**A' and 'SlKAI2**i**B' proteins. Expression analysis of the six tomato RsbQ-hydrolases showed that their expression in the roots (nonmycorrhized) is low with respect to other organs of the tomato plant (Fig. S2). Particularly, the *SlDLK2* gene is higher expressed in leaves (> five-fold) and flowers (> three-fold) than in roots (Fig. S2a).

SlDLK2 gene is induced in mycorrhizal roots

Since published data have shown that the rice KAI2 homolog *OsD14L* is required for pre-symbiotic signaling and with downstream signaling components D3 and SMAX1 also playing a role in AM symbiosis (Gutjahr *et al.*, 2015a; Choi *et al.*, 2020), we hypothesized whether SlDLK2 is similarly required for AM symbiosis.

Previous evidence identified *SlDLK2* as a highly mycorrhiza-inducible gene (García Garrido *et al.*, 2010). In this study, we show that *SlDLK2* undergoes a finely tuned regulation during arbuscular mycorrhizal development (Fig. 1a,b), with a significant induction of *SlDLK2* gene expression over time, reaching up to a 25-fold upregulation at 62 d post-inoculation (dpi) with respect to nonmycorrhizal roots (Fig. 1b).

SlDlK2 transcript levels were normalized to the AM fungal marker gene *GinEF* and, alternatively, to the plant arbuscule marker genes *SlPT4* and *RAM1* (Fig. S3). In this case, *SlDLK2* expression relativized to each one of the three marker genes did not change significantly along the mycorrhizal process, indicating that *SlDLK2* expression correlated with arbuscule formation and/or AM symbiotic function and maintenance.

In contrast to the AM-induction of the *SlDLK2* gene, expression of the other five tomato RsbQ α,β-hydrolases genes did not correlated with the mycorrhizal levels (Fig. S4). Most of these genes were unresponsive to AM inoculation, although some interesting but not significant ($0.05 > P > 1$) trends were found. For example, the *SlD14* gene, encoding the putative tomato SL receptor, seemed to be partially induced at the initial stages of mycorrhization (Fig. S4a) when SL signaling is particularly

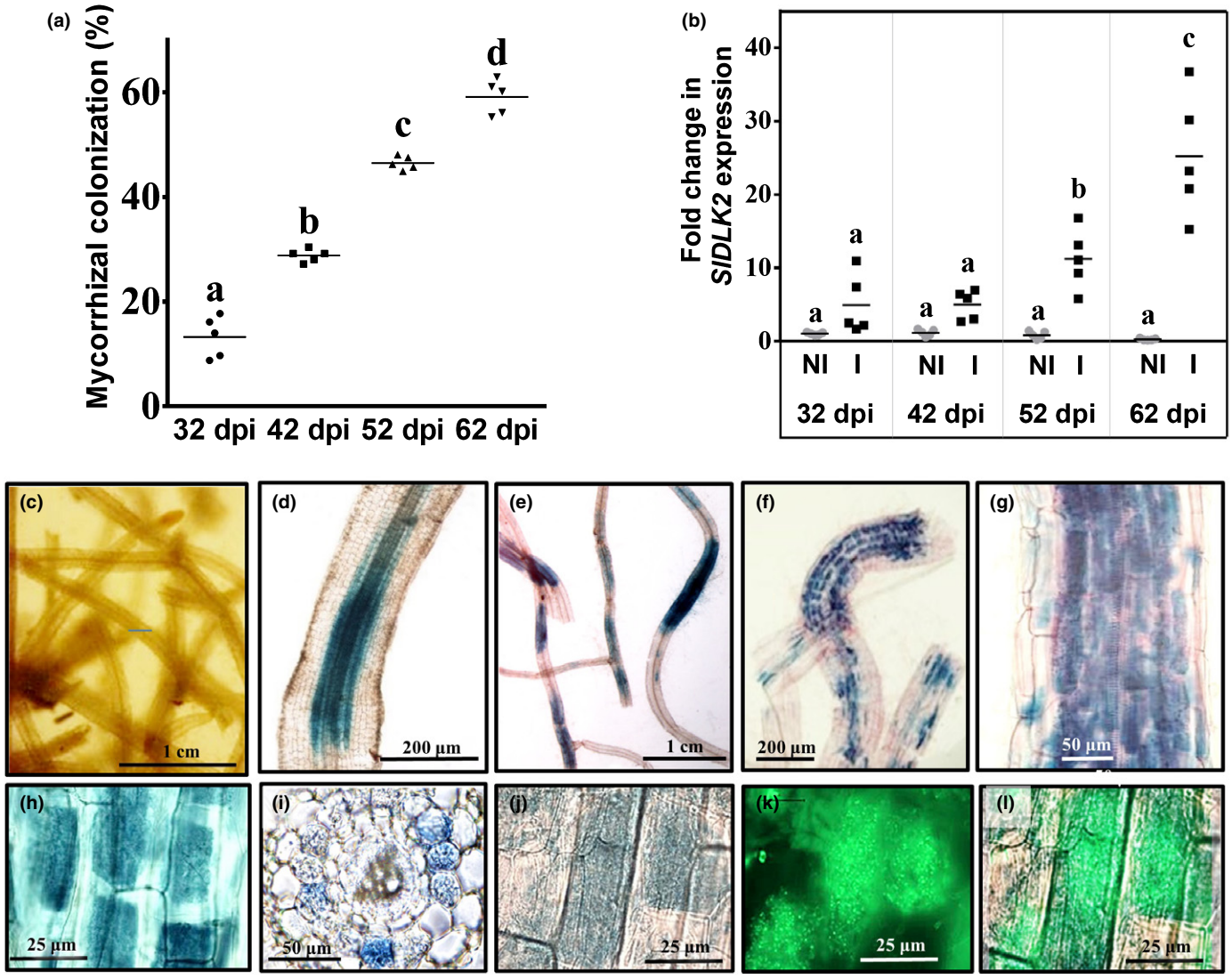

Fig. 1 Analysis of *SlDLK2* gene expression in roots. After 32, 42, 52 and 62 dpi (days post-inoculation), the percentage of total root length colonized by *Rhizophagus irregularis* was measured (a) and *SlDLK2* gene expression was analyzed by RT-qPCR (b) in noninoculated (NI) and inoculated (I) *Solanum lycopersicum* roots. RT-qPCR data represent the relative expression of the *SlDLK2* gene with respect to its expression in noncolonized plants at 32 dpi, in which its expression was designated as 1. Values correspond to mean ± SE ($n = 5$) and means denoted by a different letter indicate significant differences between treatments ($P < 0.05$). GUS activity in 8-wk-old composite tomato plants expressing the *SlDLK2* promoter *β-glucuronidase* fusion was assessed in NI roots (c, d) and mycorrhizal roots (e–l). (j–l) show a section counterstained with WGA-Alexa Fluor 488, where (j) is the bright-field image, (k) is the corresponding green fluorescent visualization of fungal structures stained with WGA-Alexa Fluor 488, and (l) is the merged image.

important for pre-symbiotic fungal growth and hyphopodium formation (Akiyama *et al.*, 2005; Kobae *et al.*, 2018). However, *SlKAI2cB*, which is one of the closest tomato orthologs to the rice KAR receptor *OsD14L* reported to be essential for mycorrhization (Gutjahr *et al.*, 2015a), had trends towards a downregulation ($0.05 > P > 0.1$) upon mycorrhization at late stages of tomato AM symbiosis (Fig. S4c).

Analysis of the *SlDLK2* promoter activity revealed that GUS activity is generally not expressed in nonmycorrhizal roots (Fig. 1c). However, unlike control roots transformed with the empty vector, which were completely unstained (Fig. S5), expression of the *SlDLK2* promoter-GUS fusion was eventually found restricted to the central cylinder (Fig. 1d), although this observation should be more deeply studied. By contrast, in mycorrhizal plants, *R. irregularis* colonization redirects *SlDLK2* expression to arbusculated cells (Fig. 1e–l), in a similar manner to the positive control roots transformed with the *SlPT4* promoter-GUS fusion (Fig. S5). Thus, *SlDLK2* expression is AM-dependent and is associated with cortex cells hosting arbuscules.

SlDLK2 negatively regulates arbuscule branching

In order to gain further insight into the function of SlDLK2 during AM establishment, we tested the effect of *SlDLK2* silencing (RNAi) and overexpression (OE) in mycorrhizal tomato roots. *SlDLK2* RNAi roots showed a significant increase both in the percentage of the root length colonized by the AM fungus

(Fig. S6a) and in all the mycorrhizal parameters (Fig. 2a) compared to the control roots. The opposite trend was observed for the *SlDLK2* OE roots (Figs S6b, 2b). Effective *SlDLK2* gene silencing or overexpression of the samples used for further analysis is shown in Fig. S6(c,d). Microscopic examination of control roots (empty vectors) and *SlDLK2* RNAi roots showed that well developed and highly branched arbuscules were abundant in these roots (Fig. 2c–g). By contrast, *SlDLK2* OE hairy roots showed remarkable alterations in arbuscular morphology (Fig. 2h–n). Undeveloped arbuscules (small, stunted, clumped and unbranched) were often found in *SlDLK2* OE mycorrhizal roots, suggesting that *SlDLK2* OE renders arbuscule branching impossible. In addition, the abundant observation of septate fungal hyphae in the cortex of *SlDLK2* OE mycorrhizal roots suggested the presence of fungal stress and degeneration.

In order to deeply study arbuscule morphology, we performed a similar analysis to that one described in Herrera-Medina *et al.* (2007). Three arbuscule classes were defined as follows: class a, arbuscules in formation (or degradation) with no fine branches and partially occupying the plant cell; class b, arbuscules with intermediate intensity of trypan blue stain occupying almost all of the plant cell; class c, arbuscules with a high intensity of trypan blue stain occupying the whole plant cell. In *SlDLK2* RNAi hairy roots, small and unbranched (class a) arbuscules were significantly less abundant, while highly intense (class c) arbuscules were overrepresented (Fig. 3a). Accordingly, the opposite phenotype was found in the *SlDLK2* OE hairy roots, with a significant increase of small and medium-size arbuscules (classes a and b), and a decrease in full-size arbuscules (class c) (Fig. 3b). Moreover, *SlDLK2* OE roots leads to a reduction in vesicle number (Fig. 3b), what is a sign of aberrant arbuscule function, as occurs in the *ram1* mutants (Pimprikar *et al.*, 2016; Luginbuehl *et al.*, 2017). Altogether, these results strongly support the idea that the arbuscule-induced gene *SlDLK2* arrests arbuscule branching.

In order to obtain additional evidence about the negative role of *SlDLK2* in arbuscule development, we decided to analyze the arbuscule activity at a molecular transcriptional level. Consistent with the increase of fully developed arbuscules in the *SlDLK2* RNAi roots, an overall upregulation of arbuscule marker genes was observed in these roots (Fig. 3c). Accordingly, the reduction in fungal colonization and the presence of abundant stunted arbuscules in *SlDLK2* OE roots was accompanied by a repression of molecular markers for arbuscule biogenesis and functioning (Fig. 3d).

In order to determine if SlDLK2 is functionally conserved in a different plant species, we performed a similar experiment on hairy roots of *Medicago truncatula*. *SlDLK2* OE in *M. truncatula* roots showed the same altered phenotype and atypical arbuscule development observed in tomato roots (Fig. S7), suggesting that *SlDLK2* OE interferes, a key general process required for arbuscular morphogenesis and development, and that DLK2 plays a widespread role in AM symbiosis.

Interestingly, the altered AM phenotype in *SlDLK2* OE roots resembles, although in a much less severe form, all the morphological features observed in the phenotype of the *Medicago* and *Lotus ram1* mutants, as well as of the petunia *ata* mutants. The ATA and RAM1 orthologs are transcription factors that act as central regulators of AM-related genes and its absence renders the AM interaction completely ineffective (Gobbato *et al.*, 2012; Rich *et al.*, 2015; Xue *et al.*, 2015).

Regulatory role of SlDLK2 in AM development

Given the AM phenotypes of the *SlDLK2* OE and RNAi plants, we hypothesized that the functional SlDLK2 protein is required to regulate arbuscule development and branching. In this scenario, SlDLK2 would act as a repressor of arbuscule branching which signals through binding to an endogenous plant or fungal ligand generated during AM symbiosis. This signaling process would require the interaction with other molecular regulators of the arbuscule life cycle. To test this hypothesis, we used two experimental approaches: (1) we determined whether SlDLK2 physically interacts with DELLA, which in turn regulates the transcription of *RAM1*, the GRAS protein required for arbuscule branching and the induction of AM marker genes (Pimprikar *et al.*, 2016), and (2) we monitored transcriptional changes directed by *SlDLK2* OE in roots using RNA sequencing.

The SlDLK2 protein has an α,β-fold core, a structure which is required for ligand reception in several related proteins such as the gibberellin, SL and KAR receptors (Shimada *et al.*, 2008; Hamiaux *et al.*, 2012; Guo *et al.*, 2013). SlDLK2 also has the conserved catalytic triad of plant SLs-receptors required for ligand binding or hydrolysis (Marzec & Brewer, 2019). In the case of the SL receptor D14, this cleavage induces the interaction of D14 with the DELLA transcription factor (Nakamura *et al.*, 2013). To test the physical interaction *in planta* between SlDLK2 and SlGAI1 (tomato DELLA), we carried out co-immunoprecipitation (coIP) assays on transient expression in *N. benthamiana* leaves. As *SlDLK2* is highly expressed in leaves (Fig. S2), we assumed that the putative ligand compound probably required for SlDLK2 activity is present in *N. benthamiana* leaves. The CoIP assay showed a physical interaction between SlDLK2 and SlGAI1 (Fig. 4a), suggesting that, like D14, SlDLK2 interacts with DELLA. Similarly, we used split-luciferase assays to demonstrate luciferase subunit complementation in the presence of tagged SlDLK2-N-luc and C-luc-SlGAI1. As for CoIP assays, the luciferase assays showed that SlDLK2 and DELLA interact in a direct manner (Fig. 4b).

To determine whether the repression of AM-marker genes by *SlDLK2* OE is due to the lower mycorrhization levels found in these roots or, by contrast, *SlDLK2* OE directly affects the downregulation of AM-related genes, we globally and independently analyzed transcriptional changes in tomato roots in response to either mycorrhizal colonization or *SlDLK2* OE (Figs S8, 5a; Tables S3, S4). An overall induction of gene expression was observed in response to mycorrhizal colonization, with 2802 induced genes and 826 downregulated genes. In noninoculated roots, the number of genes repressed (3388; 73.5%) by *SlDLK2* OE clearly exceeded the number of induced genes (1216). Surprisingly, about 42% of the genes (1176) that were found to be repressed by *SlDLK2* OE in nonmycorrhizal roots corresponded to genes upregulated in roots during mycorrhization (Fig. 5a).

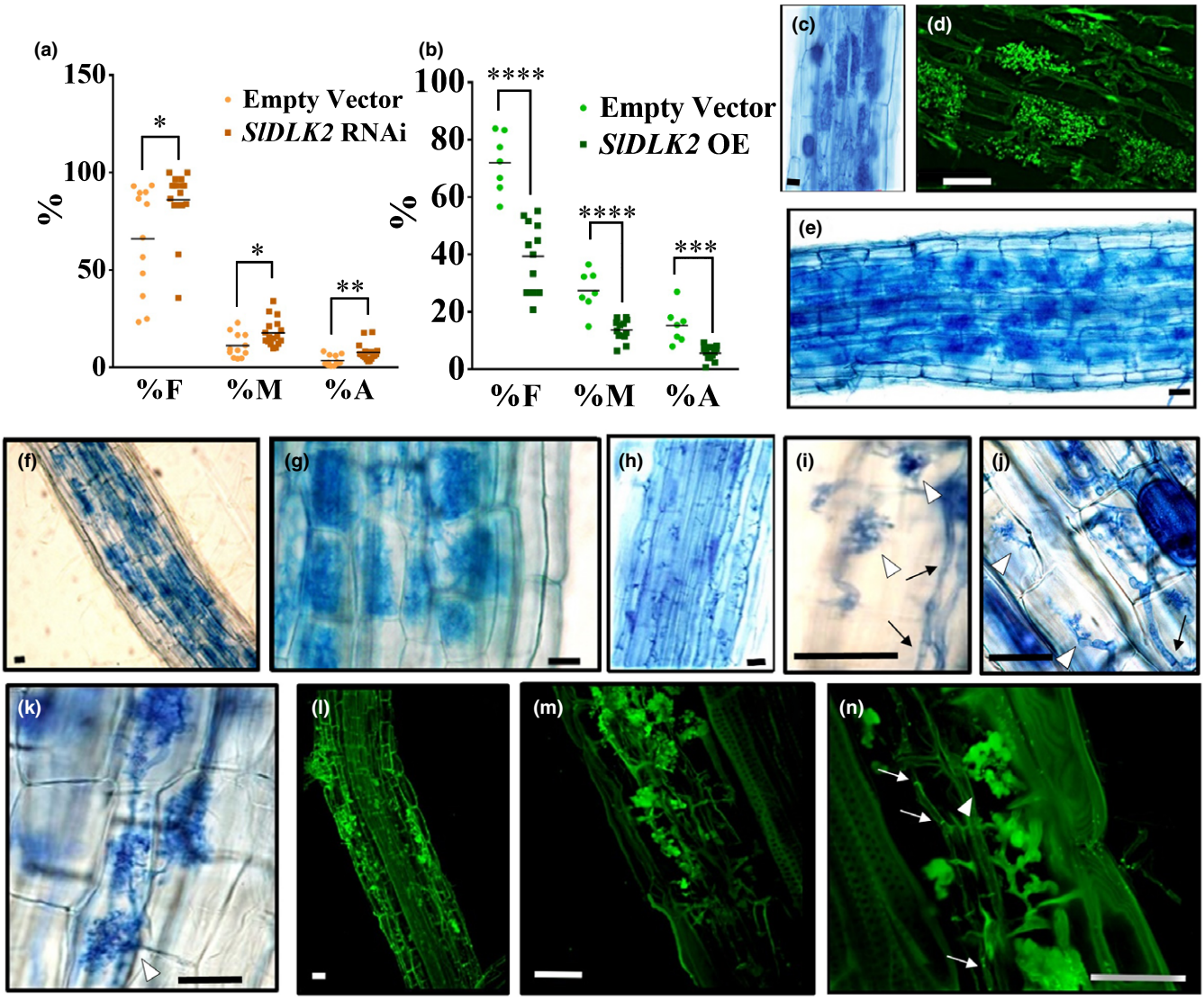

Fig. 2 Mycorrhizal phenotype of *SlDLK2* RNAi and *SlDLK2* OE composite tomato plants. (a, b) Mycorrhizal parameters (frequency, %*F*; mycorrhizal intensity, %*M*; arbuscule abundance, %*A*, in the whole root) were analyzed 50 d after inoculation with the arbuscular mycorrhizal fungus *Rhizophagus irregularis* ($n > 7$). Significant differences (Student's *t*-test) are indicated with asterisks (ns, $P > 0.1$; *, $P \leq 0.1$; **, $P \leq 0.05$; ***, $P \leq 0.01$; ****, $P \leq 0.001$). (c–n) Visualization of fungal structures in stained hairy roots transformed with the corresponding empty vectors used for overexpression (c, d) or silencing (e), the *SlDLK2* RNAi vector (f, g) and the *SlDLK2* OE vector (h–n). Tomato hairy roots were subjected to trypan blue staining or WGA-Alexa Fluor 488 and observed through light microscopy or confocal laser scanning microscopy (CLSM), respectively. Highly mycorrhized root fragments with fully developed arbuscules were observed in stained hairy roots transformed with the empty vectors or the *SlDLK2* RNAi vector (c–g). Small, stunted and clumped anomalous arbuscules with body-shaped structures (white arrowheads) were extensively appreciated in the *SlDLK2* OE plant roots, where frequent septa in the fungal hyphae appeared (white arrows). Bars, 25 μm.

These included well-known AM-marker genes involved along several stages of arbuscule life cycle (Fig. 5b), including marker genes from early stages (*CCaMK* and *Cyclops*) and developing and mature arbuscules (*Vapyrin*, *subtilase*, *EXO84*, *AMT2*, *STR* and *PT5* genes), and the regulator *RAM1*. Nevertheless, *SlDLK2* OE in nonmycorrhizal roots did not alter the expression of genes related to arbuscule degeneration (*TGL*, *Chitinase*, *PAP33* and *Cystein Protease*). The analysis of all of those marker genes in mycorrhizal roots through RT-qPCR showed an overall repression pattern of transcriptional activity upon *SlDLK2* OE (Fig. 5c) which reflects the remarkable alterations found in arbuscular morphology in these plants.

Discussion

D14 and KAI2 receptors that discriminate plant responses to SLs and KARs, respectively, belong to the RsbQ-like family of α,β-hydrolases. A third clade from this family is composed by the DLK2 (DWARF 14-LIKE2) proteins, which are structurally similar to the D14/KAI2 receptors, but whose function still remains unknown. The tomato SlDLK2 and the previously reported *Arabidopsis* DLK2 (Végh *et al.*, 2017) belong to this group. We show here that SlDLK2 (*S. lycopersicum* DWARF 14-LIKE2) is a new component involved in the complex plant-mediated signaling mechanism that regulates the life cycle of arbuscules.

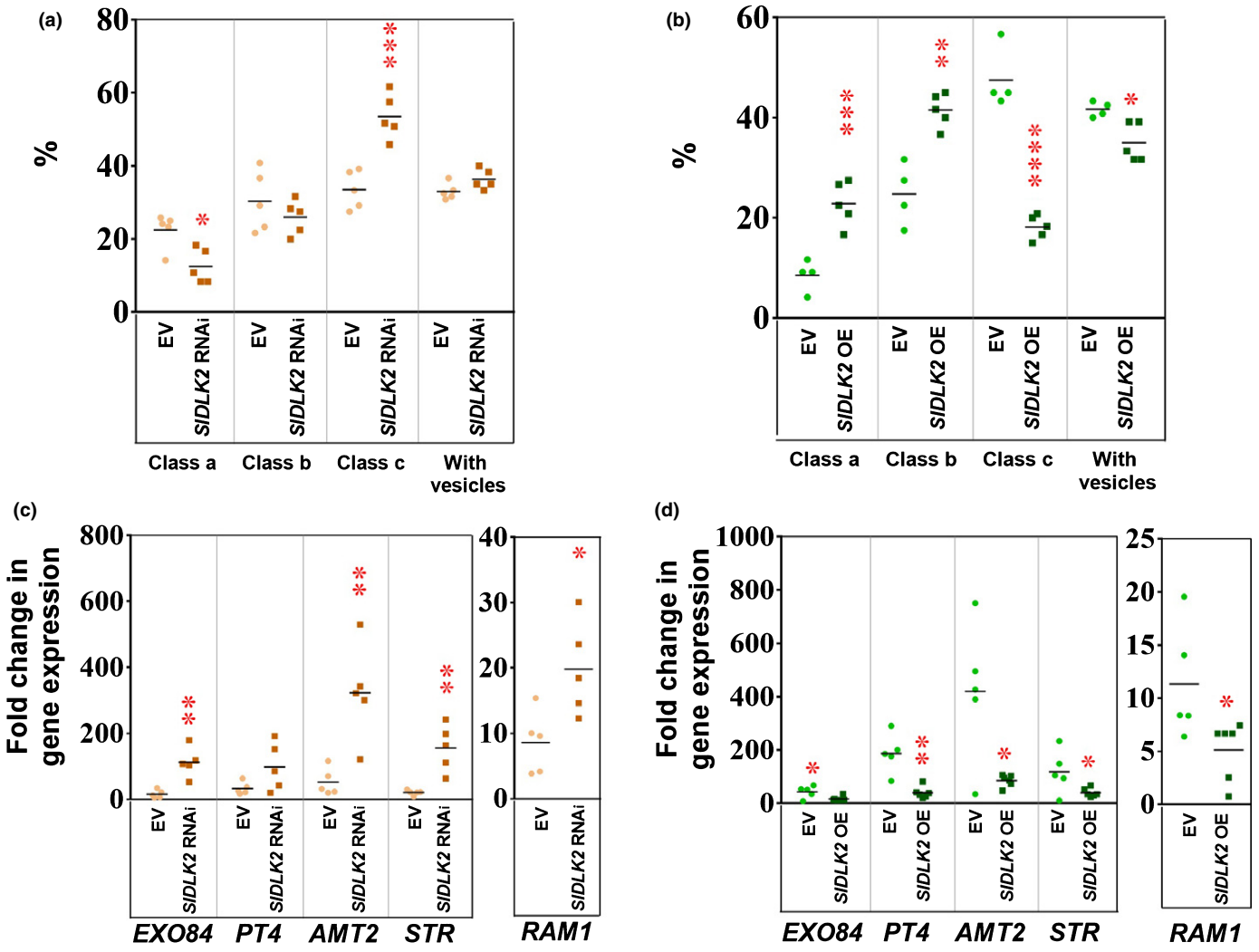

Fig. 3 Analysis of morphology and transcriptional activity of arbuscules in *SlDLK2* RNAi and *SlDLK2* OE roots. (a, b) Percentage of root intersects with a presence of vesicles and/or with a prevalence of arbuscules from three different morphological types: class a (small and unbranched), class b (middle size) or class c (highly intense occupying the whole plant cell)); in tomato composite *SlDLK2* RNAi (a) and *SlDLK2* OE (b) plants 50 d after inoculation with the arbuscular mycorrhizal fungus *Rhizophagus irregularis* ($n > 4$). (c, d) Expression of arbuscular mycorrhiza marker genes measured by RT-qPCR. RT-qPCR data represent the relative expression of the genes in mycorrhizal hairy root systems transformed with the *SlDLK2* RNAi (c) or the *SlDLK2* OE (d) vectors and the corresponding empty vectors. Expression is normalized with respect to the control noninoculated plants (not shown), in which expression was designated as 1 ($n > 5$). Values correspond to mean ± SE. Significant differences (Student's *t* test) between the plant transformed with the corresponding empty vectors (EVs) and *SlDLK2* RNAi or *SlDLK2* OE transformed plants are indicated with asterisks (*, $P < 0.05$; **, $P < 0.01$; ***, $P < 0.001$; ****, $P < 0.0001$).

In tomato, SlDLK2 plays a central role in the regulation of arbuscule branching during AM formation. The aberrant phenotype of arbuscules and the overall repression of AM-induced genes found in *SlDLK2* OE roots suggest that SlDLK2 could be a signaling receptor which triggers a signaling response that negatively regulates the mycorrhization process. The increased number of highly branched and transcriptionally active arbuscules in *SlDLK2* silenced roots strengthens this argument. Heterologous overexpression of *SlDLK2* in *M. truncatula* revealed similar results to those observed in the tomato roots, suggesting a widespread role of this receptor in AM symbiosis. In fact, previous transcriptomic analysis shows that putative orthologs of *SlDLK2* are upregulated upon mycorrhization among different AM plant species. For example, the two putative orthologs of *SlDLK2* in *Medicago*, Medtr3g045440.1 and Medtr6g086560.1, are induced during mycorrhization by 60-fold and 3.71-fold, respectively (Gomez *et al.*, 2009). In addition, the microarray data from Gutjahr *et al.* (2015b) shows that the three rice genes belonging to the DLK2 clade have a tendency towards AM-upregulation in some root types. However, further functional characterization of these putative orthologs is required to probe that *DLK2* has a conserved function and expression pattern among AM plants.

As many transcriptional changes caused by *SlDLK2* OE occurred under both inoculated and noninoculated conditions, it is reasonable to speculate that, if SlDLK2 requires a binding

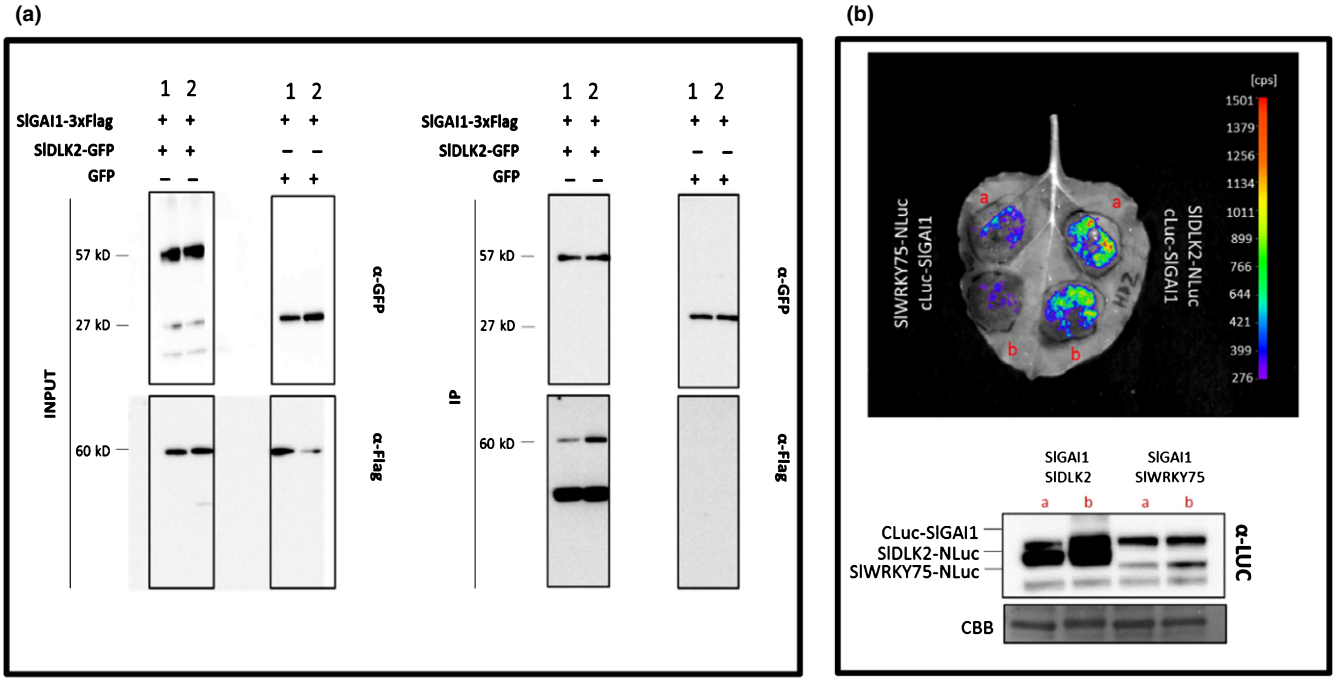

Fig. 4 SlDLK2 associates with SlGAI1 in plant cells. (a) SlDLK2-GFP or GFP was co-expressed with SlGAI1-3xFlag (dexamethasone inducible promoter) in *Nicotiana benthamiana* leaves, before immunoprecipitation using green fluorescent protein (GFP)-trap beads. SlGAI1-3xFlag was induced by dexamethasone 24 h before collecting samples. Immunoblots were analyzed using anti-GFP or anti-FLAG antibody. Molecular weight (kDa) marker bands are indicated for reference. Data for two independent experiments are shown (1 and 2). (b) LUC image of *N. benthamiana* leaf co-infiltrated with CLuc-SlGAI1 and SlDLK2-NLuc or SlWRKY75-Nluc, as negative control nuclear protein. Western blot, protein accumulation levels of CLuc- and NLuc-fusioned proteins, of *N. benthamiana* leaf are shown. Immunoblot was analyzed using anti-LUC antibody. CBB, Coomassie brilliant blue. The data shown are representative of three co-infiltrated leaves.

compound to function during mycorrhization, the corresponding ligand should be present under both mycorrhizal and nonmycorrhizal conditions. Then, it is reasonable to think that the specific ligand of SlDLK2 is neither a mycorrhizal-specific compound nor a molecule of fungal origin. Moreover, *SlDLK2* is highly expressed in leaves (Fig. S2), a DLK2 homolog is present in *Arabidopsis* which is unable to establish AM symbiosis, and the corresponding *Arabidopsis* mutant *dlk2* shows a photomorphogenic phenotype (Végh *et al.*, 2017), suggesting that DLK2 proteins have other potential functions apart from its role in AM symbiosis.

In the case of rice, the SL cleavage by D14 induces its interaction with DELLA (Nakamura *et al.*, 2013). Interestingly, we demonstrate here that SlDLK2 protein is a new DELLA interacting element. In the AM symbiosis, DELLA proteins interact with CYCLOPS and CCaMK (Sym genes) that are activated by signals from AM fungi. This interactive complex activates *RAM1* that promotes arbuscule development (Pimprikar *et al.*, 2016). This positive function of DELLA proteins in the AM symbiosis is antagonized by gibberellins (GAs). GAs are recognized by the gibberellin receptor GID1, what triggers the binding of DELLA to GID1 and the subsequent DELLA degradation. As a consequence, *RAM1* expression and arbuscule formation are inhibited. We propose a model in which the function of DELLA during mycorrhization, not only depends on GA-GID1 signaling, but also on other additional signaling compound as well as its specific α,β hydrolase-type DLK2 receptor. Although the signaling ligand that binds DLK2 is completely unknown, we speculate that as D14 binds the apocarotenoid molecule SL, DLK2 might bind another apocarotenoid-type compound. In fact, the methylerythritol phosphate (MEP) pathway, which is responsible for apocarotenoid synthesis, is activated in mycorrhizal roots (Walter *et al.*, 2007), and some C13 and C14 apocarotenoid compounds with unknown function have been reported to accumulate in mycorrhizal roots (Klingner *et al.*, 1995; Maier *et al.*, 1995). According to this model, specific apocarotenoids-SlDLK2 recognition promotes SlDLK2–DELLA interactions that interfere with the role of DELLA as an activator of the transcription of RAM1, which, in turn, triggers the formation of arbuscules (Fig. 6). It is established that RAM1 is a master regulator of arbuscule development, as it is required for the activation of AM-genes related to arbuscule functioning (Pimprikar *et al.*, 2016; Rich *et al.*, 2017). Then, the aberrant arbuscule phenotype, the abundant septate fungal hyphae and the decreased number of vesicles in *SlDLK2* OE roots resemble the phenotype of *ram1* mutants (Gobbato *et al.*, 2012; Rich *et al.*, 2015; Xue *et al.*, 2015), and might be due to a direct effect of *SlDLK2* OE on *RAM1* repression from the earliest stages of arbuscule formation. However, *RAM1* induction is probably not limited to the formation of arbuscules and might be extended to later stages, in active and developed arbuscules, being required to maintain arbuscular functionality. This is supported by previous promoter-GUS analyzes showing that *RAM1* promoters from tomato and *Lotus* are also expressed in apparently mature arbuscules (Pimprikar *et al.*, 2016;

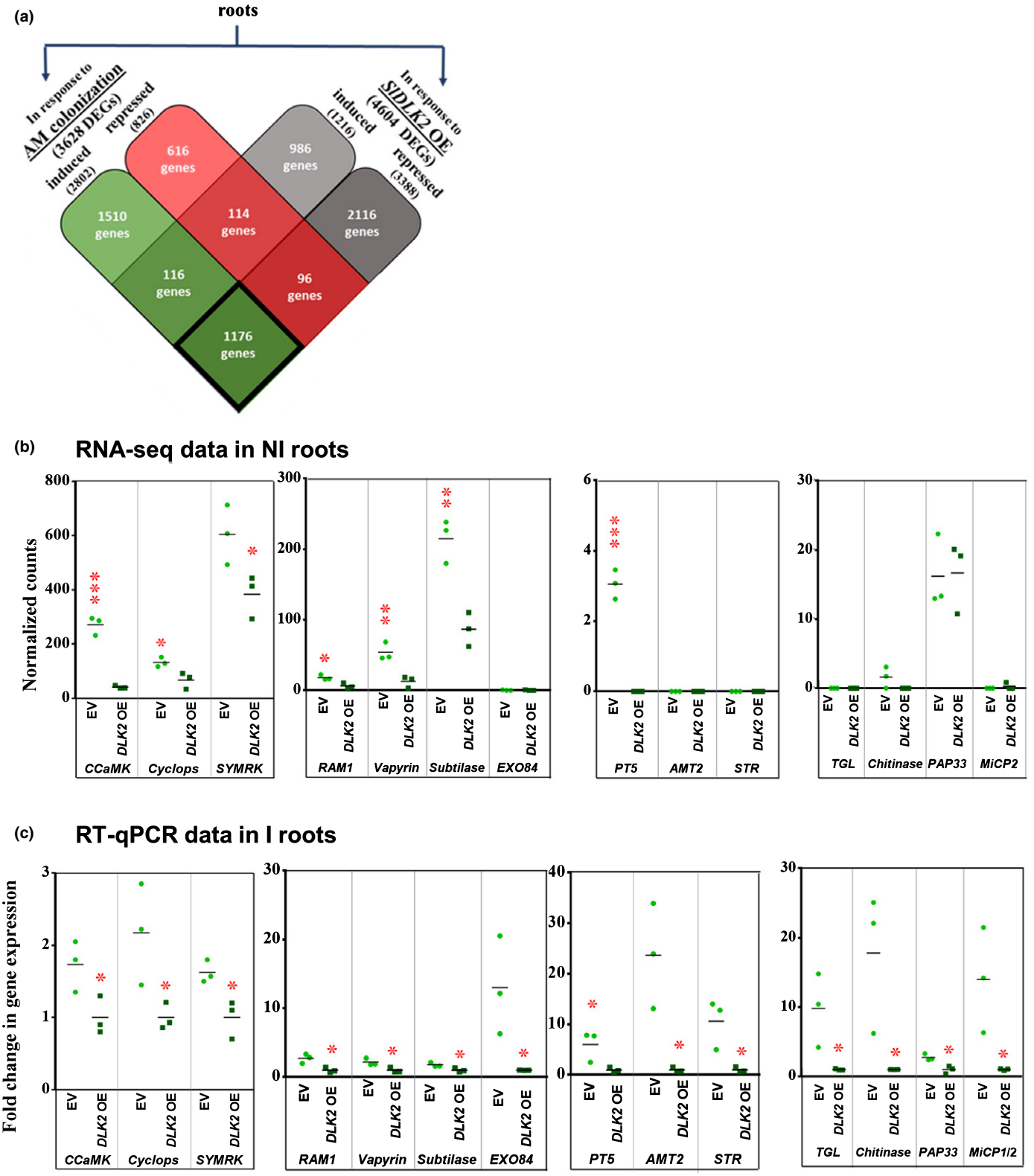

Fig. 5 *SlDLK2* overexpression regulates arbuscular mycorrhiza (AM)-related genes in nonmycorrhizal and mycorrhizal roots. (a) Diagram depicting the number of differentially expressed genes (DEGs) significantly induced or repressed ($P < 0.05$ and fold change > 2 or < −2, respectively) in nonmycorrhizal roots upon either mycorrhization or *SlDLK2* OE. (b) Expression of AM-related genes in response to *SlDLK2* OE in nonmycorrhizal roots, expressed as normalized counts by DEseq: Genes from the Common Symbiosis Signaling Pathway (*CCaMK*, *Cyclops* and *SYMRK*), arbuscule-related genes (*RAM1*, *Vapyrin*, *Subtilase*, *EXO84*, *PT5*, *AMT2* and *STR*) and putative arbuscule-degeneration maker genes (*TGL*, *Chitinase*, *PAP33* and *MiCP*). (c) Expression of the same AM-related genes in response to *SlDLK2* OE in mycorrhizal roots, measured by RT-qPCR. RT-qPCR data represent the relative gene expression with respect to the *SlDLK2* OE plants in which its expression was designated as 1. Values correspond to mean ± SE ($n = 3$). Significant differences (Student's *t* test) between the mutant and the control are indicated with asterisks (*, $P < 0.05$; **, $P < 0.01$; ***, $P < 0.001$).

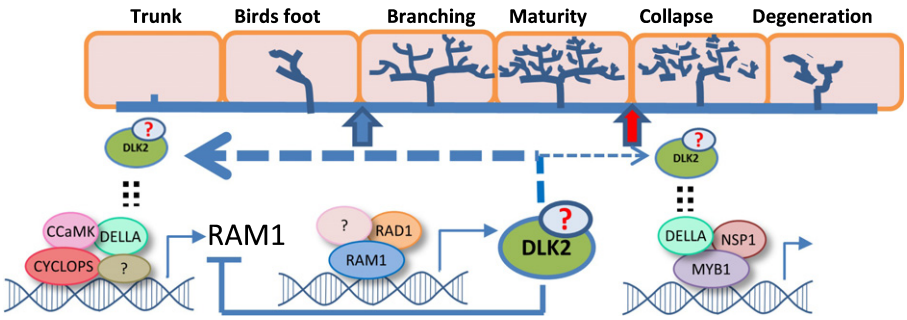

Fig. 6 Proposed model of participation of DLK2 in the regulation of arbuscule life cycle. In a heterocomplex with DELLA protein, CYCLOPS and CCaMK regulate the expression of *RAM1*. RAM1 transcription factor is able to interact with several other GRAS-domain proteins (such as RAD1) and activates the expression of genes involved in arbuscule development and functioning. As a consequence of arbuscular activity, *DLK2* transcription is activated and DLK2 protein would bind an unidentified ligand. MYB1 is required for the transcriptional regulation of genes involved in arbuscule degeneration and interacts with both DELLA and the GRAS-domain protein NSP1. The important role of DELLA in arbuscule development, thorough RAM1, and collapse, through MYB1, raise the question of whether SlDLK2 is a suppressor of arbuscule development or a positive regulator of arbuscule degeneration. The proposed model suggests that DLK2 regulates arbuscule development rather than collapse and it is based on DLK2 capacity to bind DELLA, its nonability to induce transcription of senescence gene expression and its direct negative effect on mycorrhization genes, including *RAM1* transcription (thick continuous line). However, we cannot totally rule out the possibility that DLK2 is also involved in the degeneration of arbuscules (fine dotted arrow). The different stages of arbuscule development are shown. The blue and red arrowheads delimited the beginning of RAM1 and MYB1 activity, respectively.

Ho-Plágaro *et al.*, 2019). Moreover, the expression of RAM1-dependent genes occurs during arbuscule formation but it is also typical of functionally active and well developed arbuscules, what suggests that *RAM1* expression is not restricted to arbuscules in a developing stage. In this sense, we hypothesize that *DLK2* induction is kept in mature arbuscules, in the same manner as other symbiotic genes. When a certain amount of DLK2 protein (and probably also its required ligand) is reached, DLK2 binds DELLA, so available DELLA for *RAM1* activation is reduced, and then all RAM1-dependent genes are also repressed, with the resulting inhibition of arbuscule branching and activity. Overall, our results strongly suggest that the DLK2 α,β-hydrolase plays a role during late stages of arbuscule development, particularly in the autoregulation of arbuscule branching and functioning (Fig. 6). This is a remarkable finding as, to date, studies concerning D14L protein and D14-mediated SL signaling have only shown a role of RsbQ α,β-hydrolases at early stages of AM symbiosis, i.e. during pre-symbiotic signaling.

Nevertheless, DELLA protein is also involved in the degeneration of arbuscules, and it has described the existence of a transcription regulatory complex formed by DELLA and NSP1 which, together with the transcription factor MYB1 (MYB-like family), form a regulatory module for the transcription of genes encoding proteins with hydrolytic activity (proteases, chitinases, etc.) associated with the process of arbuscular degeneration (Floss *et al.*, 2017). Therefore, the DELLA protein is involved both in the formation and the degeneration of arbuscules depending on the different transcription regulatory complexes formed. In this scenario, we cannot rule out the possibility that SlDLK2 is involved in the degeneration of arbuscules, and thus, *SlDLK2* OE would cause accelerated arbuscule collapse rather than conditioning arbuscule development. However, results presented here, showing an overall repression pattern of transcriptional activity of those hydrolytic marker genes in mycorrhizal roots upon *SlDLK2* OE, clearly point to a role of SlDLK2 as a negative regulator of arbuscule development, rather than an inductor of arbuscule degradation. Future experiments will be aimed at unveiling the meaning of the DELLA–SlDLK2 interaction on the regulation of arbuscule branching in infected cells.

Acknowledgements

We thank Michael O'Shea for proof-reading the document; G. Marco (Sistemas Genómicos, Valencia, Spain) for technical assistance in bioinformatics and statistical analysis of the RNA-seq data; and Jose S. Rufián for biochemical advice. Tania Ho-Plágaro was supported by a research fellowship from the FPI-MINECO program. This study was supported by grants from the Comisión Interministerial de Ciencia y Tecnología (CICYT) and Fondos Europeos de Desarrollo Regional (FEDER) through the Ministerio de Economía, industria y Competitividad in Spain (AGL2014-52298-P, AGL2017-83871-P), and Shanghai Center for Plant Stress Biology (Chinese Academy of Sciences) and the Chinese 1000 Talents program.

Author contributions

TH-P, RJLM, APM, JAL-R and JMG-G designed the study and discussed the experiments. TH-P, MIT-N, RJLM, RH and NM-R performed the experiments. TH-P and JMG-G wrote the manuscript with assistance of other authors.

ORCID

José Manuel García-Garrido https://orcid.org/0000-0001-9420-8926
Raúl Huertas https://orcid.org/0000-0003-0147-0752
Juan Antonio López-Ráez https://orcid.org/0000-0001-7973-9251
Alberto P. Macho https://orcid.org/0000-0001-9935-8026
Rafael J. L. Morcillo https://orcid.org/0000-0002-0546-5195

References

Akiyama K, Matsuzaki K, Hayashi H. 2005. Plant sesquiterpenes induce hyphal branching in arbuscular mycorrhizal fungi. *Nature* **435**: 824–827.

Akiyama K, Ogasawara S, Ito S, Hayashi H. 2010. Structural requirements of strigolactones for hyphal branching in AM fungi. *Plant & Cell Physiology* **51**: 1104–1117.

Anders S, Huber W. 2010. Differential expression analysis for sequence count data. *Genome biology* **11**: R106.

Anders S, Pyl PT, Huber W. 2015. HTSeq—a Python framework to work with high-throughput sequencing data. *Bioinformatics* **31**: 166–169.

Bennett T, Liang Y, Seale M, Ward S, Müller D, Leyser O. 2016. Strigolactone regulates shoot development through a core signalling pathway. *Biology Open* **5**: 1806–1820.

Chabot S, Bécard G, Piché Y. 1992. Life cycle of *Glomus intraradix* in root organ culture. *Mycologia* **84**: 315–321.

Choi J, Lee T, Cho J, Servante EK, Pucker B, Summers W, Bowden S, Rahimi M, An K, An G. 2020. The negative regulator SMAX1 controls mycorrhizal symbiosis and strigolactone biosynthesis in rice. *Nature Communications* **11**: 1–13.

Delaux PM, Xie X, Timme RE, Puech-Pages V, Dunand C, Lecompte E, Delwiche CF, Yoneyama K, Becard G, Sejalon-Delmas N. 2012. Origin of strigolactones in the green lineage. *New Phytologist* **195**: 857–871.

Flematti GR, Ghisalberti EL, Dixon KW, Trengove RD. 2004. A compound from smoke that promotes seed germination. *Science* **305**: 977.

Floss DS, Gomez SK, Park H-J, MacLean AM, Müller LM, Bhattarai KK, Lévesque-Tremblay V, Maldonado-Mendoza IE, Harrison MJ. 2017. A transcriptional program for arbuscule degeneration during AM symbiosis is regulated by MYB1. *Current Biology* **27**: 1206–1212.

García Garrido JM, León Morcillo RJ, Martín Rodríguez JA, Ocampo Bote JA. 2010. Variations in the mycorrhization characteristics in roots of wild-type and ABA-deficient tomato are accompanied by specific transcriptomic alterations. *Molecular Plant–Microbe Interactions* **23**: 651–664.

Gobbato E, Marsh JF, Vernié T, Wang E, Maillet F, Kim J, Miller JB, Sun J, Bano SA, Ratet P. 2012. A GRAS-type transcription factor with a specific function in mycorrhizal signaling. *Current Biology* **22**: 2236–2241.

Gomez SK, Javot H, Deewatthanawong P, Torres-Jerez I, Tang Y, Blancaflor EB, Udvardi MK, Harrison MJ. 2009. *Medicago truncatula* and *Glomus intraradices* gene expression in cortical cells harboring arbuscules in the arbuscular mycorrhizal symbiosis. *BMC Plant Biology* **9**: 10.

Gomez-Roldan V, Fermas S, Brewer PB, Puech-Pagès V, Dun EA, Pillot J-P, Letisse F, Matusova R, Danoun S, Portais J-C. 2008. Strigolactone inhibition of shoot branching. *Nature* **455**: 189.

Guo Y, Zheng Z, La Clair JJ, Chory J, Noel JP. 2013. Smoke-derived karrikin perception by the alpha/beta-hydrolase KAI2 from Arabidopsis. *Proceedings of the National Academy of Sciences, USA* **110**: 8284–8289.

Gutjahr C, Gobbato E, Choi J, Riemann M, Johnston MG, Summers W, Carbonnel S, Mansfield C, Yang SY, Nadal M *et al.* 2015a. Rice perception of symbiotic arbuscular mycorrhizal fungi requires the karrikin receptor complex. *Science* **350**: 1521–1524.

Gutjahr C, Sawers RJ, Marti G, Andrés-Hernández L, Yang S-Y, Casieri L, Angliker H, Oakeley EJ, Wolfender J-L, Abreu-Goodger C. 2015b. Transcriptome diversity among rice root types during asymbiosis and interaction with arbuscular mycorrhizal fungi. *Proceedings of the National Academy of Sciences, USA* **112**: 6754–6759.

Hamiaux C, Drummond RS, Janssen BJ, Ledger SE, Cooney JM, Newcomb RD, Snowden KC. 2012. DAD2 is an alpha/beta hydrolase likely to be involved in the perception of the plant branching hormone, strigolactone. *Current Biology* **22**: 2032–2036.

Herrera-Medina MJ, Steinkellner S, Vierheilig H, Ocampo Bote JA, García Garrido JM. 2007. Abscisic acid determines arbuscule development and functionality in the tomato arbuscular mycorrhiza. *New Phytologist* **175**: 554–564.

Hewitt EJ. 1966. *Sand and water culture methods used in the study of plant nutrition.* Farnham Royal, UK: Commenwealth Agricultural Bureaux.

Ho-Plágaro T, Huertas R, Tamayo-Navarrete MI, Ocampo JA, García-Garrido JM. 2018. An improved method for *Agrobacterium rhizogenes*-mediated transformation of tomato suitable for the study of arbuscular mycorrhizal symbiosis. *Plant Methods* **14**: 34.

Ho-Plágaro T, Molinero-Rosales N, Flores DF, Díaz MV, García-Garrido JM. 2019. Identification and expression analysis of GRAS transcription factor genes involved in the control of arbuscular mycorrhizal development in tomato. *Frontiers in Plant Science* **10**: 268.

Hosmani PS, Flores-Gonzalez M, van de Geest H, Maumus F, Bakker LV, Schijlen E, van Haarst J, Cordewener J, Sanchez-Perez G, Peters S. 2019. An improved de novo assembly and annotation of the tomato reference genome using single-molecule sequencing, Hi-C proximity ligation and optical maps. *bioRxiv*. 767764.

Jefferson R. 1989. The GUS reporter gene system. *Nature* **342**: 837.

Kagiyama M, Hirano Y, Mori T, Kim SY, Kyozuka J, Seto Y, Yamaguchi S, Hakoshima T. 2013. Structures of D14 and D14L in the strigolactone and karrikin signaling pathways. *Genes to Cells* **18**: 147–160.

Karimi M, Inze D, Depicker A. 2002. GATEWAY vectors for *Agrobacterium*-mediated plant transformation. *Trends in Plant Science* **7**: 193–195.

Klingner A, Bothe H, Wray V, Marner F-J. 1995. Identification of a yellow pigment formed in maize roots upon mycorrhizal colonization. *Phytochemistry* **38**: 53–55.

Kobae Y, Kameoka H, Sugimura Y, Saito K, Ohtomo R, Fujiwara T, Kyozuka J. 2018. Strigolactone biosynthesis genes of rice is required for the punctual entry of arbuscular mycorrhizal fungi into the roots. *Plant and Cell Physiology* **59**: 544–553.

Koltai H, LekKala SP, Bhattacharya C, Mayzlish-Gati E, Resnick N, Wininger S, Dor E, Yoneyama K, Yoneyama K, Hershenhorn J. 2010. A tomato strigolactone-impaired mutant displays aberrant shoot morphology and plant interactions. *Journal of Experimental Botany* **61**: 1739–1749.

Kretzschmar T, Kohlen W, Sasse J, Borghi L, Schlegel M, Bachelier JB, Reinhardt D, Bours R, Bouwmeester HJ, Martinoia E. 2012. A petunia ABC protein controls strigolactone-dependent symbiotic signalling and branching. *Nature* **483**: 341.

Kryvoruchko IS, Sinharoy S, Torres-Jerez I, Sosso D, Pislariu CI, Guan D, Murray J, Benedito VA, Frommer WB, Udvardi MK. 2016. *MtSWEET11*, a nodule-specific sucrose transporter of *Medicago truncatula*. *Plant Physiology* **171**: 554–565.

Kumar S, Stecher G, Tamura K. 2016. MEGA7: molecular evolutionary genetics analysis version 7.0 for bigger datasets. *Molecular Biology and Evolution* **33**: 1870–1874.

Li X. 2011. Infiltration of *Nicotiana benthamiana* protocol for transient expression via *Agrobacterium*. *Bio-protocol* **1**: e95.

Livak KJ, Schmittgen TD. 2001. Analysis of relative gene expression data using real-time quantitative PCR and the $2^{-\Delta\Delta CT}$ method. *Methods* **25**: 402–408.

López-Ráez JA, Verhage A, Fernandez I, Garcia JM, Azcón-Aguilar C, Flors V, Pozo MJ. 2010. Hormonal and transcriptional profiles highlight common and differential host responses to arbuscular mycorrhizal fungi and the regulation of the oxylipin pathway. *Journal of Experimental Botany* **61**: 2589–2601.

Luginbuehl LH, Menard GN, Kurup S, Van Erp H, Radhakrishnan GV, Breakspear A, Oldroyd GE, Eastmond PJ. 2017. Fatty acids in arbuscular mycorrhizal fungi are synthesized by the host plant. *Science* **356**: 1175–1178.

Luginbuehl LH, Oldroyd GE. 2017. Understanding the arbuscule at the heart of endomycorrhizal symbioses in plants. *Current Biology* **27**: R952–R963.

Machin DC, Hamon-Josse M, Bennett T. 2020. Fellowship of the rings: a saga of strigolactones and other small signals. *New Phytologist* **225**: 621–636.

MacLean AM, Bravo A, Harrison MJ. 2017. Plant signaling and metabolic pathways enabling arbuscular mycorrhizal symbiosis. *The Plant Cell* **29**: 2319–2335.

Maier W, Peipp H, Schmidt J, Wray V, Strack D. 1995. Levels of a terpenoid glycoside (blumenin) and cell wall-bound phenolics in some cereal mycorrhizas. *Plant Physiology* **109**: 465–470.

Marzec M, Brewer P. 2019. Binding or hydrolysis? How does the strigolactone receptor work? *Trends in Plant Science* **24**: 571–574.

Mindrebo JT, Nartey CM, Seto Y, Burkart MD, Noel JP. 2016. Unveiling the functional diversity of the alpha/beta hydrolase superfamily in the plant kingdom. *Current Opinion in Structural Biology* **41**: 233–246.

Nakamura H, Xue Y-L, Miyakawa T, Hou F, Qin H-M, Fukui K, Shi X, Ito E, Ito S, Park S-H. 2013. Molecular mechanism of strigolactone perception by DWARF14. *Nature Communications* **4**: 2613.

Nelson DC, Flematti GR, Riseborough J-A, Ghisalberti EL, Dixon KW, Smith SM. 2010. Karrikins enhance light responses during germination and seedling development in *Arabidopsis thaliana*. *Proceedings of the National Academy of Sciences, USA* **107**: 7095–7100.

Phillips JM, Hayman D. 1970. Improved procedures for clearing roots and staining parasitic and vesicular-arbuscular mycorrhizal fungi for rapid assessment of infection. *Transactions of the British Mycological Society* **55**: 158IN116–161IN118.

Pimprikar P, Carbonnel S, Paries M, Katzer K, Klingl V, Bohmer MJ, Karl L, Floss DS, Harrison MJ, Parniske M. 2016. A CCaMK-CYCLOPS-DELLA complex activates transcription of *RAM1* to regulate arbuscule branching. *Current Biology* **26**: 987–998.

Pimprikar P, Gutjahr C. 2018. Transcriptional regulation of arbuscular mycorrhiza development. *Plant and Cell Physiology* **59**: 673–690.

Rich MK, Courty PE, Roux C, Reinhardt D. 2017. Role of the GRAS transcription factor *ATA/RAM1* in the transcriptional reprogramming of arbuscular mycorrhiza in *Petunia hybrida*. *BMC Genomics* **18**: 589.

Rich MK, Schorderet M, Bapaume L, Falquet L, Morel P, Vandenbussche M, Reinhardt D. 2015. The petunia GRAS transcription factor *ATA/RAM1* regulates symbiotic gene expression and fungal morphogenesis in arbuscular mycorrhiza. *Plant Physiology* **168**: 788–797.

Sang Y, Wang Y, Ni H, Cazalé AC, She YM, Peeters N, Macho AP. 2018. The *Ralstonia solanacearum* type III effector RipAY targets plant redox regulators to suppress immune responses. *Molecular Plant Pathology* **19**: 129–142.

Shimada A, Ueguchi-Tanaka M, Nakatsu T, Nakajima M, Naoe Y, Ohmiya H, Kato H, Matsuoka M. 2008. Structural basis for gibberellin recognition by its receptor GID1. *Nature* **456**: 520–523.

Sievers F, Wilm A, Dineen D, Gibson TJ, Karplus K, Li W, Lopez R, McWilliam H, Remmert M, Soding J *et al.* 2011. Fast, scalable generation of high-quality protein multiple sequence alignments using Clustal Omega. *Molecular Systems Biology* **7**: 539.

Smith S, Read D. 2008. *Mycorrhizal symbiosis. 3rd edn.* London, UK: Academic Press.

Stirnberg P, Furner IJ, Ottoline Leyser H. 2007. MAX2 participates in an SCF complex which acts locally at the node to suppress shoot branching. *The Plant Journal* **50**: 80–94.

Stirnberg P, van De Sande K, Leyser HO. 2002. MAX1 and MAX2 control shoot lateral branching in *Arabidopsis*. *Development* **129**: 1131–1141.

Sun YK, Flematti GR, Smith SM, Waters MT. 2016. Reporter gene-facilitated detection of compounds in *Arabidopsis* leaf extracts that activate the Karrikin signaling pathway. *Frontiers in Plant Science* **7**: 1799.

Trapnell C, Pachter L, Salzberg SL. 2009. TopHat: discovering splice junctions with RNA-Seq. *Bioinformatics* **25**: 1105–1111.

Trapnell C, Williams BA, Pertea G, Mortazavi A, Kwan G, Van Baren MJ, Salzberg SL, Wold BJ, Pachter L. 2010. Transcript assembly and quantification by RNA-Seq reveals unannotated transcripts and isoform switching during cell differentiation. *Nature Biotechnology* **28**: 511–515.

Trouvelot A. 1986. Mesure du taux de mycorhization VA d'un systeme radiculaire. Recherche de methodes d'estimation ayant une significantion fonctionnelle. Mycorrhizae: physiology and genetics: 217–221.

Umehara M, Hanada A, Magome H, Takeda-Kamiya N, Yamaguchi S. 2010. Contribution of strigolactones to the inhibition of tiller bud outgrowth under phosphate deficiency in rice. *Plant and Cell Physiology* **51**: 1118–1126.

Végh A, Incze N, Fábián A, Huo H, Bradford KJ, Balázs E, Soós V. 2017. Comprehensive analysis of DWARF14-LIKE2 (DLK2) reveals its functional divergence from strigolactone-related paralogs. *Frontiers in Plant Science* **8**: 1641.

Vogel JT, Walter MH, Giavalisco P, Lytovchenko A, Kohlen W, Charnikhova T, Simkin AJ, Goulet C, Strack D, Bouwmeester HJ. 2010. SlCCD7 controls strigolactone biosynthesis, shoot branching and mycorrhiza-induced apocarotenoid formation in tomato. *The Plant Journal* **61**: 300–311.

Walter MH, Floß DS, Hans J, Fester T, Strack D. 2007. Apocarotenoid biosynthesis in arbuscular mycorrhizal roots: contributions from methylerythritol phosphate pathway isogenes and tools for its manipulation. *Phytochemistry* **68**: 130–138.

Wang L, Xu Q, Yu H, Ma H, Li X, Yang J, Chu J, Xie Q, Wang Y, Smith SM. 2020. Strigolactone and karrikin signaling pathways elicit ubiquitination and proteolysis of SMXL2 to regulate hypocotyl elongation in Arabidopsis. *The Plant Cell* **32**: 2251–2270.

Wang Y, Li Y, Rosas-Diaz T, Caceres-Moreno C, Lozano-Duran R, Macho AP. 2018. The IMMUNE-ASSOCIATED NUCLEOTIDE-BINDING 9 protein is a regulator of basal immunity in *Arabidopsis thaliana*. *Molecular Plant–Microbe Interactions* **32**: 65–75.

Waters MT, Nelson DC, Scaffidi A, Flematti GR, Sun YK, Dixon KW, Smith SM. 2012. Specialisation within the DWARF14 protein family confers distinct responses to karrikins and strigolactones in *Arabidopsis*. *Development* **139**: 1285–1295.

Xue L, Cui H, Buer B, Vijayakumar V, Delaux P-M, Junkermann S, Bucher M. 2015. Network of GRAS transcription factors involved in the control of arbuscule development in *Lotus japonicus*. *Plant Physiology* **167**: 854–871.

Yoshida S, Kameoka H, Tempo M, Akiyama K, Umehara M, Yamaguchi S, Hayashi H, Kyozuka J, Shirasu K. 2012. The D3 F-box protein is a key component in host strigolactone responses essential for arbuscular mycorrhizal symbiosis. *New Phytologist* **196**: 1208–1216.

Supporting Information

Additional Supporting Information may be found online in the Supporting Information section at the end of the article.

Fig. S1 Phylogenetic analysis of the RsbQ-like family of α,β-hydrolase folds.

Fig. S2 Expression analysis of the Rsb-Q-like α,β-hydrolase gene family in tomato.

Fig. S3 Expression of *SlDLK2* gene relativized to fungal colonization and AM function marker genes.

Fig. S4 Tomato RsbQ-like α,β-hydrolases gene expression pattern in mycorrhizal roots.

Fig. S5 GUS staining of *Solanum lycopersicum* hairy roots transformed with the empty vector or with the *SlPT4* promoter::GUS fusion.

Fig. S6 *SlDLK2* gene expression and mycorrhizal colonization in hairy roots of *SlDLK2* RNAi and OE AM composite plants.

Fig. S7 *Medicago truncatula* hairy roots overexpressing *SlDLK2* are impaired in proper arbuscule formation.

Fig. S8 Validation of RNAseq data analysis by RT-qPCR.

Table S1 Primers used in this study for PCR amplifications and plasmid constructions.

Table S2 Primers used in this study for quantitative reverse transcription polymerase chain reaction (RT-qPCR) experiments.

Table S3 Number of mapped reads, high quality reads and splices reads for libraries from each sample in the RNA-seq analysis.

Table S4 List of DEGs genes.

Please note: Wiley Blackwell are not responsible for the content or functionality of any Supporting Information supplied by the authors. Any queries (other than missing material) should be directed to the *New Phytologist* Central Office.